Int. J. Nano Dimens. 6 (4): 385-398, Autumn 2015
ISSN: 2008-8868

Contents list available at **IJND**

International Journal of Nano Dimension

Journal homepage: *www.IJND.ir*

Evaluation of the heat transfer rate increases in retention pools nuclear waste

D. Domari Ganji*
M. M. Peiravi
M. Abbasi

Department of Mechanical Engineering, Islamic Azad University, Sari Branch, Sari, Iran.

Received 25 November 2014
Received in revised form
10 January 2015
Accepted 18 January 2015

* Corresponding author:
Davood Domari Ganji
Department of Mechanical Engineering, Islamic Azad University, Sari Branch, Sari, Iran.
Tel +98 1133375061
Fax +98 1133365061
Email *ddg_davood@yahoo.com*

ABSTRACT

In this paper, we have tried to find a solution for quick transfer of nuclear wastes from pools of cool water to dry stores to reduce the environmental concerns and financial cost of burying atomic waste. Therefore, the rate of heat transfer from atomic waste materials to the outer surface of the container should be increased. This can be achieved by covering the bottom of the pool space with conical fins (vertically) embedded in porous medium and allowing natural convection flow of Newtonian nanofluid upon it. In this research, we studied the rate of heat transfer by using such special space. In this study, Heat transfer boundary layer flow in Nano-fluidics shifting from a vertical cone in porous medium, two-dimensional, steady, incompressible and low speed flow have been considered and attempts have been made to obtain analytical solutions for it. The obtained nonlinear ordinary differential equation has been solved through homotopy analysis method (HAM), considering boundary conditions and Nusselt number. Also, Nusselt number, which is an important parameter in heat transfer, is calculated using the obtained analytical solution by HAM. A comparison of the obtained analytical solution with the numerical results represented a remarkable accuracy. The results also indicate that HAM can provide us with a convenient way to control and adjust the convergence region.

Keywords: *Nuclear wastes; Homotopy analysis method (HAM); Porous media; Newtonian nanofluid; Similarity solution; Ordinary differential equations (ODE).*

INTRODUCTION

Natural convection flow of fluid over a surface embedded in saturated porous media is encountered in many engineering problems, such as the design of pebble-bed nuclear reactors, ceramic processing, crude oil drilling, geothermal energy conversion, use of fibrous material in the thermal insulation of buildings, catalytic reactors and compact heat exchangers, heat transfer from storage of agricultural products which generate heat as a result of metabolism, petroleum reservoirs, storage of nuclear wastes.

In nuclear industry, the consumed atomic fuels (nuclear wastes) are generally stored protectively in specially designed small pools, in which the uranium is cooled by water to prevent it from exiting radioactive radiations. After several decades of protective storage in the pools, the temperature and radiation by the fuel are reduced noticeably, after which it is removed from the small pools and transferred into metallic or concrete containers for dry storing. However, even in this phase of storage, the radiations by fuels are still dangerous and can cause safety concerns. Depending on the type of fuel, reduction in temperature and radiations from the fuel to reach the standard level during this protective storage phase can vary from several years to decades. According to Andrew Kadak, a researcher from the Massachusetts Institute of Technology (MIT), USA, the consumed fuel, instead of transferring to disposal dump, has the potential to become a big source of energy, comparable to the large strategic oil stores. Storage of consumed fuel in dry reservoirs for several decades to cool the fuel to safe temperature and then bury it in a permanent burying dump can be cheaper and managed in smaller space if the consumed fuel can be retrieved and reproduced. In this research, we tried to find a solution for quick transfer of atomic dump from pools of cool water to dry stores by increasing heat transfer from atomic waste materials to outside surface of the container. This was achieved by covering the bottom of the pool with conical fins embedded (vertically) in porous medium and allowing natural convection flow of Newtonian nanofluid upon it. The approach, using such specially designed space, is expected not only to reduce the environmental concerns, but also the financial expenses of burying atomic waste considerably.

The derivation of the empirical equations which govern the flow and heat transfer in a porous medium has been discussed in [1]. The natural convection on vertical surfaces in porous media has been studied used Darcy's law by a number of authors [2–4]. Boundary layer analysis of natural convection over a cone has been investigated by Yih [5]. Murthy and Singh [6] obtained the similarity solution for non-Darcy mixed convection about an isothermal vertical cone with fixed apex half angle, pointing downwards in a fluid saturated porous medium with uniform free stream velocity, but a semi-similar solution of an unsteady mixed convection flow over a rotating cone in a rotating viscous fluid has been obtained Roy and Anilkumar [7].The laminar steady nonsimilar natural convection flow of gases over an isothermal vertical cone has been investigated by Takhar et al. [8]. The development of unsteady mixed convection flow of an incompressible laminar viscous fluid over a vertical cone has been investigated by Singh and Roy [9] when the fluid in the external stream is set into motion impulsively, and at the same time the surface temperature is suddenly changed from its ambient temperature. An analysis has been carried out by Kumari and Nath [10] to study the non-Darcy natural convention flow of Non-Newtonian fluids on a vertical cone embedded in a saturated porous medium with power-law variation of the wall temperature/concentration or heat/mass flux and suction/ injection. Cheng [11] focused on the problem of natural convection from a vertical cone in a porous medium with mixed thermal boundary conditions, Soret and Dufour effects and with variable viscosity. The conventional heat transfer fluids including oil, water and ethylene glycol etc. are poor heat transfer fluids, since the thermal conductivity of these fluids play an important role on the heat transfer coefficient between the heat transfer medium and the heat transfer surface. An innovative technique for improving heat transfer by using ultra fine solid particles in the fluids has been used extensively during the last several years. Choi [12] introduced the term non-Newtonian nanofluid refers to these kinds of fluids by suspending nanoparticles in the base fluid. Khanafer et al. [13] investigated the heat transfer enhancement in a two-dimensional enclosure utilizing nanofluids. The convective boundary-layer flow over vertical plate, stretching sheet and moving surface studied by numerous studies and in the review papers Buongiorno [14], Daungthongsuk and Wongwises [15], Oztop [16], Nield and Kuznetsov [17,18], Ahmad and Pop [19], Khan and Pop [20], Kuznetsov and Nield [21,22] and Bachok et al. [23]. From literature survey the base aim of this work is to study the free convection boundary layer flow past a vertical cone embedded in a porous medium filled with a nanofluid, the basic fluid being a Newtonian fluid by using similarity transformations. The ordinary differential equations are solved homotopy analysis method (HAM). The

effects of the parameters governing the problem are studied and discussed.

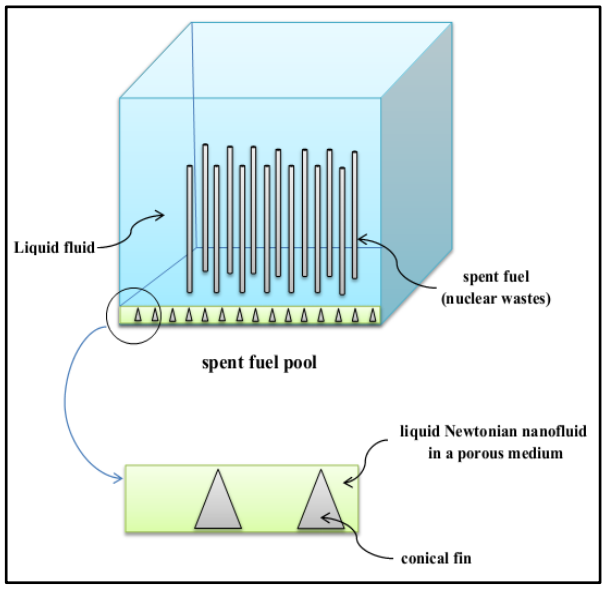

Fig. 1. Bottom of the spent fuel pool

Consider the problem of natural convection about a downward -pointing vertical cone of half angle γ embedded in a porous medium saturated with a Newtonian power-law nanofluid (Figure 1). The origin of the coordinate system is placed at the vertex of the full cone, with x being the coordinate along the surface of the cone measured from the origin and y being the coordinate perpendicular to the conical surface Figure 2. The temperature of the porous medium on the surface of the cone is kept at constant temperature T_w , and the ambient porous medium temperature is held at constant temperature T_∞ .The nanofluid properties are assumed to be constant except for density variations in the buoyancy force term. The thermo physical properties of the Newtonian nanofluid are given in Table 1. Assuming that the thermal boundary layer is sufficiently thin compared with the local radius, the equations governing the problem of Darcy flow through a homogeneous porous medium saturated with power-law Newtonian nanofluid near the vertical cone can be written in two-dimensional Cartesian coordinates (x, y) as:

$$\frac{\partial\left(r^a u\right)}{\partial x}+\frac{\partial\left(r^a v\right)}{\partial y}=0 \qquad (1)$$

$$u=\frac{(\rho\beta)_{nf}}{\mu_{nf}}K_d\, g\,(T-T_\infty)\cos\varphi \qquad (2)$$

$$u\frac{\partial T}{\partial x}+v\frac{\partial T}{\partial y}=\left(\frac{k}{\rho c_p}\right)_{nf}\frac{\partial^2 T}{\partial y^2} \qquad (3)$$

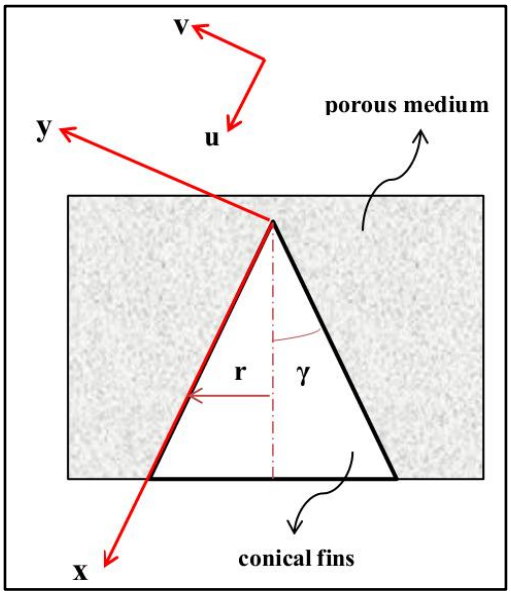

Fig. 2. A schematic diagram of the physical model

Where u and v are the volume-averaged velocity components in the x and y directions, respectively, T is the volume-averaged temperature and g is the gravitational acceleration. a= γ =0 corresponds to flow over a vertical flat plate and a= γ =1 corresponds to flow over a vertical cone Property ρ_{nf} and μ_{nf} are the density and effective viscosity of the nanofluid, and K_d is the modified permeability of the porous medium. Furthermore, α_{nf} and β_{nf} are the equivalent thermal diffusivity and the thermal expansion coefficient of the saturated porous medium, which are defined as:

$$\begin{aligned}
\rho_{nf} &= (1-\phi)\rho_f + \phi\rho_s \\
\mu_{nf} &= \frac{\mu_f}{(1-\phi)^{2.5}} \\
\alpha_{nf} &= \frac{k_{nf}}{\left(\rho c_p\right)_{nf}} \\
\left(\rho c_p\right)_{nf} &= (1-\phi)\left(\rho c_p\right)_f + \phi\left(\rho c_p\right)_s
\end{aligned} \qquad (4)$$

$$\frac{k_{nf}}{k_f}=\frac{\left(k_s+2k_f\right)-2\phi\left(k_f-k_s\right)}{\left(k_s+2k_f\right)+2\phi\left(k_f-k_s\right)}$$

Table 1. Thermo-physical properties of water and nanoparticles

Number	Material	Physical properties			
		ρ (kg/m^3)	C_P (J/KgK)	k (W/mK)	$\beta x10^5$ (k^{-1})
1	*Pure water*	997.1	4179	0.613	21
2	*Copper (Cu)*	8933	385	401	1.67
3	*Silver (Ag)*	10500	235	429	1.89
4	*Alumina (Al_2O_3)*	3970	765	40	0.85
5	*Titanium (TiO_2)*	4250	686.2	8.9538	0.9

Here ϕ is the solid volume fraction.
The associated boundary conditions of (1)-(3) can be written as:

$$\begin{aligned} &u = 0\ ;\quad T \to T_\omega \quad \text{as} \quad y \to \infty \\ &v = 0\ ;\quad T = T_\omega \quad \text{at} \quad y = 0 \end{aligned} \tag{5}$$

Where μ_f is the viscosity of the basic fluid, ρ_f and ρ_s are the densities of the pure fluid and nanoparticle, respectively, $(\rho Cp)_f$ and $(\rho Cp)_s$ are the specific heat parameters of the base fluid and nanoparticle, respectively, k_f and k_s are the thermal conductivities of the base fluid and nanoparticle, respectively. The local radius to a point in the boundary layer r can be represented by the local radius of the vertical cone r=xsinγ. By introducing the following non-dimensional variables:

$$\eta = \frac{y}{x} Ra_x^{\ 0.5}$$

$$f(\eta) = \frac{\psi(x,y)}{\alpha_f\, r^a Ra_x^{\ 0.5}} \tag{6}$$

$$\theta(\eta) = \frac{T - T_\infty}{T_w - T_\infty}$$

The continuity equation is automatically satisfied by defining a stream function $\Psi(x,y)$ such that:

$$r^a u = \frac{\partial(\psi)}{\partial y} \quad , \quad r^a v = -\frac{\partial(\psi)}{\partial x} \tag{7}$$

Where;

$$Ra_x = \left(\frac{x}{\alpha_f}\right)\left[\frac{(\beta\rho)_f\ gK_d\cos\varphi\Delta T}{\mu_f}\right] \tag{8}$$

Integration the momentum (2) we have:

$$\frac{\mu_{nf}}{\mu_f} u = \frac{(\rho\beta)_{nf}\ K_d\, g\cos\varphi}{\mu_f}(T - T_\infty) \tag{9}$$

Substituting variables (6) into (1)–(5) with (9), we obtain the following system of ordinary differential equations:

$$\frac{1}{(1-\phi)^{2.5}\left[(1-\phi)+\phi\frac{(\rho\beta)_s}{(\rho\beta)_f}\right]} f'(\eta) = \theta(\eta) \tag{10}$$

$$\frac{\left(\frac{(k_s+2k_f)-2\phi(k_f-k_s)}{(k_s+2k_f)+2\phi(k_f-k_s)}\right)}{\left((1-\phi)+\phi\frac{(\rho c_p)_s}{(\rho c_p)_f}\right)}\theta''(\eta)+\left(\frac{1}{2}+a\right) f(\eta)\theta'(\eta) = 0 \tag{11}$$

Along with the boundary conditions:

$$\begin{aligned} &f(0) = 0 \quad , \quad \theta(0) = 1 \\ &f'(\infty) = 0 \quad , \quad \theta'(\infty) = 0 \end{aligned} \tag{12}$$

Finally from (10)-(12) we have:

$$\text{ODE:}\ \left(\frac{1}{2}+a\right)\left((1-\phi)+\phi\frac{(\rho c_p)_s}{(\rho c_p)_f}\right) f(\eta) f''(\eta) + \left(\frac{(k_s+2k_f)-2\phi(k_f-k_s)}{(k_s+2k_f)+2\phi(k_f-k_s)}\right) f'''(\eta) = 0 \tag{13}$$

$$\text{B.C:}\ f(0) = 0\ ,\ f'(0) = 1\ ,\ f'(\infty) = 0 \tag{14}$$

It is of interest to obtain the value of the local Nusselt number which is defined as:

$$Nu_x = \frac{q_w\, x}{k\,(T_w - T_\infty)} \tag{15}$$

Where q_w for the case of prescribed wall temperature can be computed from:

$$q_w = -k \left.\frac{\partial T}{\partial y}\right|_{y=0} \quad (16)$$

From (15), (16), (6) and (8) it follows that the local Nusselt number is given by:

$$Nu_x = Ra_x^{0.5}\left[-\theta'(0)\right] \quad (17)$$

EXPERIMENTAL

Computational Method

Consider governing equation of Newtonian nanofluid flow and heat transfer of cone embedded in porous medium that is expressed by (13) to Consideration boundary conditions. Consider equation that prescribed wall temperature case that is expressed by (13). We define a nonlinear operator as follow:

$$N\left[f(\eta;q)\right] = \left(\frac{1}{2}+a\right)\left((1-\phi)+\phi\frac{(\rho c_p)_s}{(\rho c_p)_f}\right) f(\eta;q)\frac{\partial^2 f(\eta;q)}{\partial\eta^2} + \left(\frac{(k_s+2k_f)-2\phi(k_f-k_s)}{(k_s+2k_f)+2\phi(k_f-k_s)}\right)\frac{\partial^3 f(\eta;q)}{\partial\eta^3} \quad (18)$$

Where, qε [0, 1] the embedding parameter, $\hbar \neq 0$ is a nonzero auxiliary parameter. As the embedding parameter increases from 0 to 1, *U(η,q)* varies from the initial guess $U_0(\eta)$ to the exact solution *U(η)*;

$$f(\eta;0) = U_0(\eta) \quad , \quad f(\eta;1) = U(\eta) \quad (19)$$

Expanding *f (η,q)* in Taylor series with respect to q, we have:

$$f(\eta;q) = U_0(\eta) + \sum_{m=1}^{+\infty} U_m(\eta) q^m \quad (20)$$

Where

$$U_m(\eta) = \frac{1}{m!}\left.\frac{\partial^m f(\eta;q)}{\partial q^m}\right|_{p=0} \quad (21)$$

Homotopy analysis method can be expressed by many different base functions [24-28], according to the governing equation; it is straightforward to use a set of base functions:

$$\left\{\eta^p e^{-m\eta} \,|\, p, m = 0,1,2,3,\ldots\right\} \quad (22)$$

In the form

$$U(\eta) = \sum_{m=1}^{\infty}\sum_{p=1}^{\infty} b_p \eta^p e^{-m\eta} \quad (23)$$

That bn is a coefficient to be determined. Besides determining a set of base function, the auxiliary function *H(η),* initial approximation $U_0(\eta)$ and the auxiliary linear operator *L* must be chosen in such a way that all solutions of the corresponding high-order deformation equations exist and can be express by this set of the base function and the other expressions such as $\eta^n \sin(m\eta)$ must be avoided. This provides us with the so-called rule of solution expression [29]. It should be noticed that term like $\eta^p e^{-m\eta}|p,\ m > 0$ does not belong to the so-called secular terms such as ($\eta^p\sin(m\eta)$, $\eta^p\cos(m\eta)$) because the term $\eta^p e^{-m\eta}|p,\ m > 0$ tend zero as $\eta\to\infty$ [29]. We choose linear operator, as below:

$$L\left[f(\eta;q)\right] = \frac{\partial^3 f(\eta;q)}{\partial\eta^3} \quad (24)$$

With the property

$$L\left[c_1 + c_2\eta + c_3 e^{-\eta}\right] = 0 \quad (25)$$

Where, c_1, c_2 and c_3 are integral constants. We must choose initial guess of *U(η)* so that it prevents divergence of answers. According to the discussed limitation and under the rule of solution expression and initial conditions we choose initial guess in form:

$$U_0(\eta) = c_1 + c_2\eta + c_3 e^{-\eta} \quad (26)$$

$$U_0(\eta) = 1 - \exp(-\eta) \quad (27)$$

$$(1-q)L\left[f(\eta;q)-U_0(s)\right]=qhH(s)N\left[f(\eta;q)\right] \quad (28)$$

$$f(0;q)=0\ ,\ \frac{\partial f(\infty;q)}{\partial\eta}=0\ ,\ \frac{\partial^2 f(\infty;q)}{\partial\eta^2}=0 \quad (29)$$

According to the rule of solution expression denoted by (24) and from (28), the auxiliary function *H(η)* can be chosen as follows:

$$H(\eta)=\eta^p e^{m\eta} \quad (30)$$

Differentiating (28), m times with respect to the embedding parameter q and then setting q = 0 and finally dividing them by m! and From (19), (26) We have the so-called mth-order deformation equation for m≥1:

$$U_m(\eta)=\chi_m U_{m-1}(\eta)+\hbar\int_0^{\eta}\int_0^{\mu}\int_0^{\tau}H(\eta)e^{\eta}R_m\left(\vec{U}_{m-1}\right)d\eta d\tau d\mu+c_1+c_2\eta+c_3e^{-\eta}$$

$$U_m(0)=0\ ,\ (U_m)'(\infty)=0\ ,\ (U_m)''(\infty)=0 \quad (31)$$

Where

$$R_m\left(\vec{U}_{m-1}\right)=\left(\frac{(k_s+2k_f)-2\phi(k_f-k_s)}{(k_s+2k_f)+2\phi(k_f-k_s)}\right)\frac{\partial^3\vec{U}_{m-1}(\eta)}{\partial\eta^3}+\left(\frac{1}{2}+a\right)\left((1-\phi)+\phi\frac{(\rho c_p)_s}{(\rho c_p)_f}\right)\left(\sum_{z=0}^{m-1}\vec{U}_z(\eta)\left(\frac{\partial^2\vec{U}_{m-1-z}(\eta)}{\partial\eta^2}\right)\right) \quad (32)$$

And

$$\chi_m=\begin{cases}0, & m\le 1,\\ 1, & m>1\end{cases} \quad (33)$$

It's time to choose *H(η)* uniquely under the rule of solution expression and rule of coefficient ergodicity [29]. So we have to choose {p = 0, m = -1}. Consequently the corresponding auxiliary function was determined uniquely $H(\eta)=e^{-\eta}$. We now successively obtain:

$$U_0(\eta)=1-e^{-\eta} \quad (34)$$

The zero order deformation equation is:

$$\begin{aligned}U_1(\eta)=&\left(-0.05711939723+0.06126805522\,e^{-1.x}+0.007293506583\,e^{-3.x}\right.\\&-0.008242682212\,e^{-4.x}-0.01193332704\,e^{-5.x}\\&-0.001904150650\,e^{-6.x}+0.01071045486\,e^{-2.x}\\&\left.-0.00007245953384\,e^{-7.x}\right)h^3+\left(-0.2740431288\right.\\&-0.004137625704\,e^{-5.x}-0.05846724927\,e^{-4.x}\\&+0.05802396765\,e^{-2.x}+0.3486814590\,e^{-1.x}\\&\left.-0.07005742290\,e^{-3.x}\right)h^2+\left(-0.5422444335\right.\\&+1.001446451\,e^{-1.x}-0.3761596017\,e^{-2.x}\\&\left.-0.08304241593\,e^{-3.x}\right)h+1.-1.\,e^{-x}\end{aligned}$$

We should ensure that the solution converges. Note that we still have freedom to choose the auxiliary parameter *ħ*, as pointed by Liao [29], the convergence region and rate of solution series can be adjusted and controlled by means of the auxiliary parameter *ħ*. In general, by means of the so-called ħ-curve, it is straightforward to choose an appropriate range for *ħ* which ensures the convergence of the solution series. To influence of *ħ* on the convergence of solution, we plot the so-called ħ-curves of f(η), by 17th-order approximation of solution for Cu-water, Ag-water, Al_2O_3-water and TiO_2-water in ϕ =0.1, as shown in Figures 3- 6. It is easy to discover the valid region of *ħ* is -1.5≤ħ≤0. Moreover, increasing the order of approximation increases the range of acceptable values of *ħ*.

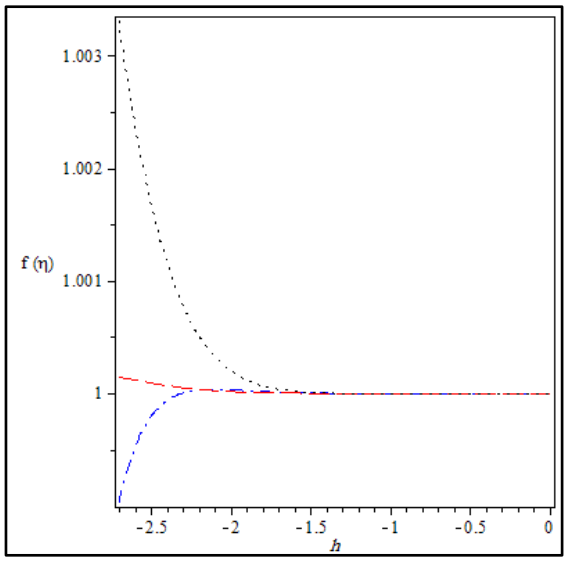

Fig. 3. The h-curve by 17th-order approximation for Cu-water . Γ=0.1

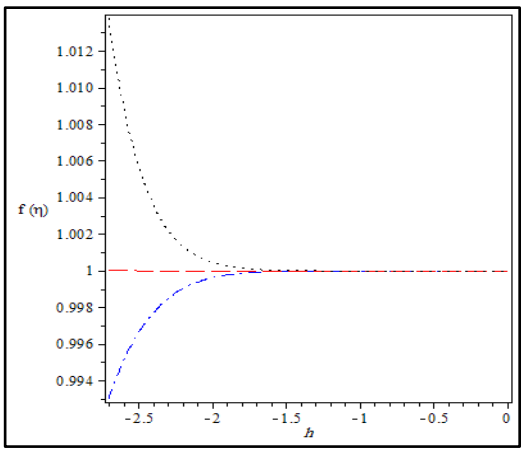

Fig. 4. The h-curve by 17th-order approximation for Ag-water. Γ=0.1.

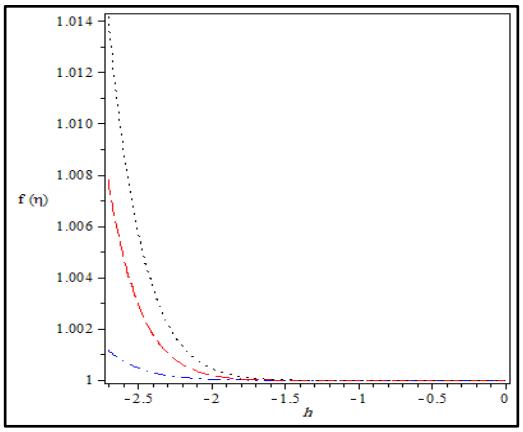

Fig. 5 . The h-curve by 17th-order approximation for Al_2O_3-water. Γ=0.1

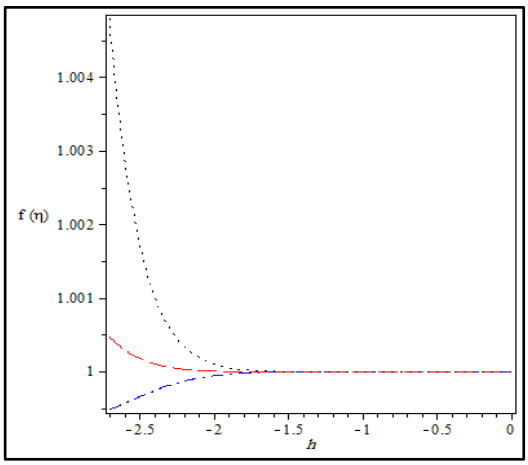

Fig. 6 . The h-curve by 17th-order approximation for TiO_2-water. Γ=0.1

RESULTS AND DISCUSSION

In this study we have presented similarity reductions for the effect of a nanoparticle volume fraction on the free convection flow of nanofluids over a vertical cone via similarity transformations. The homotopy analysis method (HAM) solutions of the resulted similarity reductions are obtained for the original variables which are shown in (13) along with the boundary conditions (14) by using the homotopy analysis method (HAM). The physical quantity of interest here is the Nusselt number Nu_x and it is obtained and shown in (17). The distributions of the velocity $f(\eta)$, $\theta(\eta)$ and the Nusselt number in the cases of Cu-water, Ag-water, Al_2O_3-water and TiO_2-water are shown in Figures 7–18. The computations are carried for various values of the nanoparticles volume fraction for different types of nanoparticles, when the base fluid is water. Nanoparticles volume fraction ϕ is varied from 0 to 0.25. The nanoparticles used in the study are from Copper (Cu), Silver (Ag), Alumina (Al_2O_3) and Titanium oxide (TiO_2). Table 2 depict the heat transfer rate $\theta'(0)$ for various values of nanoparticles volume fraction ϕ for different types of nanoparticles when the base fluid is water. Figures show the effects of the nanoparticle volume fraction γ on the velocity distribution in the cases of Cu-water, Ag-water, Al_2O_3-water and TiO_2-water when ϕ = 0, 0.025, 0.05, 0.075, 0.1, 0.125, 0.15, 0.175, 0.2, 0.225, 0.25. It is noted that the velocity along the cone increases with the nanoparticle volume fraction in the four cases, moreover the velocity distribution in the case of Ag-water is larger than that for Cu-water, Al_2O_3-water and TiO_2-water. We can show that the changes of the velocity distribution when we use different types of nanoparticles from Figures 7-10, which depict the Ag-nanoparticles, are the highest when the base fluid is water. Thus the presence of the nanoparticles volume fraction increases the momentum boundary layer thickness.

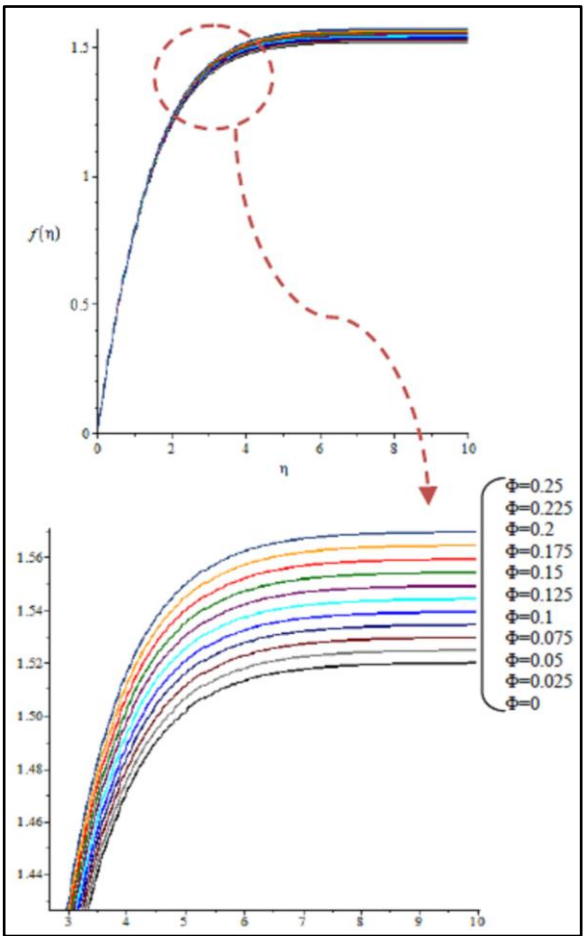

Fig. 7. Effect of ϕ on velocity distribution *f (η)* in the case of Ag-water

Table 2. Values of *-θ'(0)* for various values of ϕ.

ϕ	Material			
	Copper (Cu)	*Silver (Ag)*	*Alumina (Al_2O_3)*	*Titanium (TiO_2)*
0.025	0.4557512	0.45465451	0.4557379	0.45706440
0.05	0.4549851	0.45279643	0.4549496	0.45761224
0.075	0.4542139	0.45093107	0.4541517	0.45814745
0.1	0.4534526	0.44906030	0.4533546	0.45867323
0.125	0.4526836	0.44718110	0.4525424	0.45918932
0.15	0.4519008	0.44529991	0.4517311	0.45969944
0.175	0.4511371	0.44342033	0.4509225	0.46018894
0.2	0.4503621	0.44152570	0.4501101	0.46067544

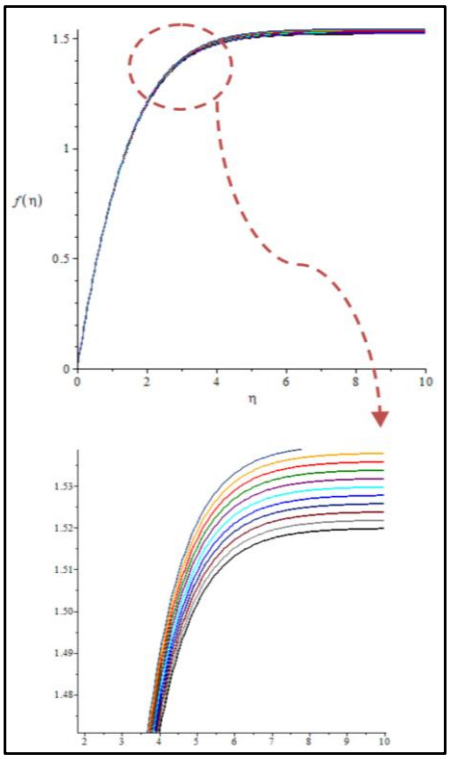

Fig. 8. Effect of ϕ on velocity distribution *f (η)* in the case of Cu-water

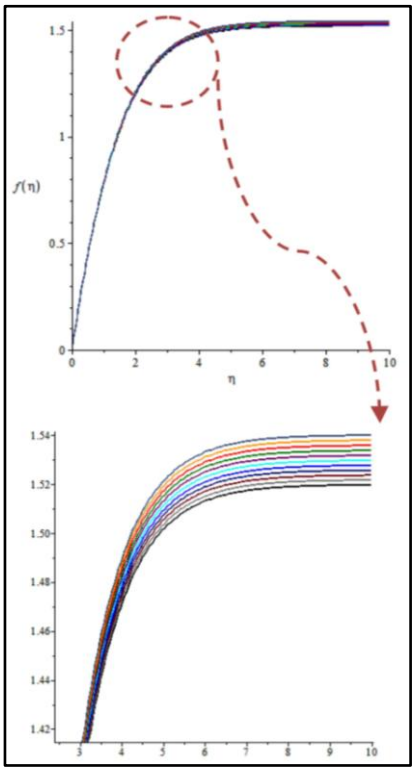

Fig. 9. Effect of ϕ on velocity distribution *f (η)* in the case of Al_2O_3-water

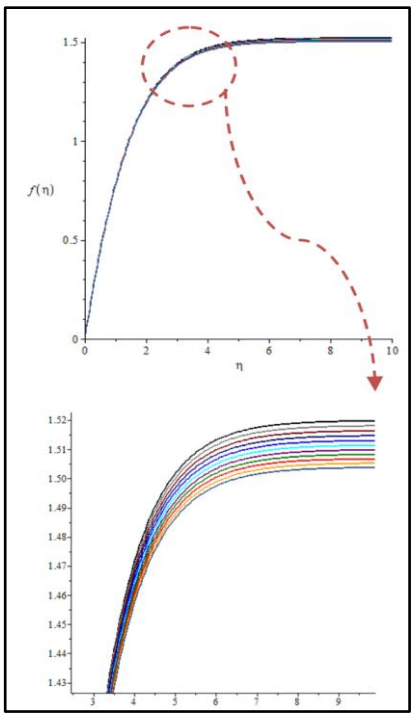

Fig. 10. Effect of ϕ on velocity distribution *f (η)* in the case of TiO_2-water

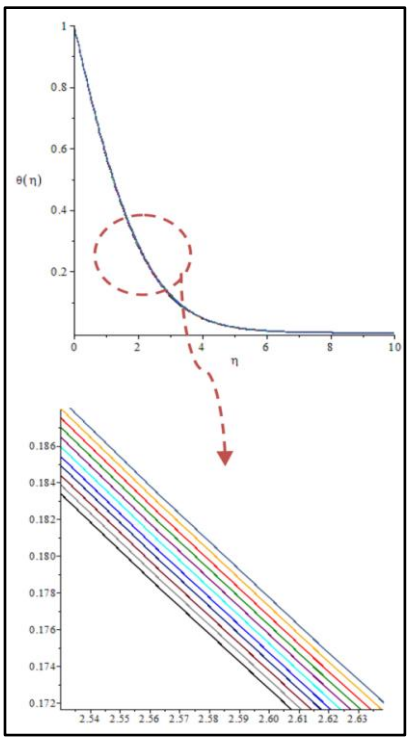

Fig. 12. Effect of ϕ on velocity distribution *θ(η)* in the case of Cu-water

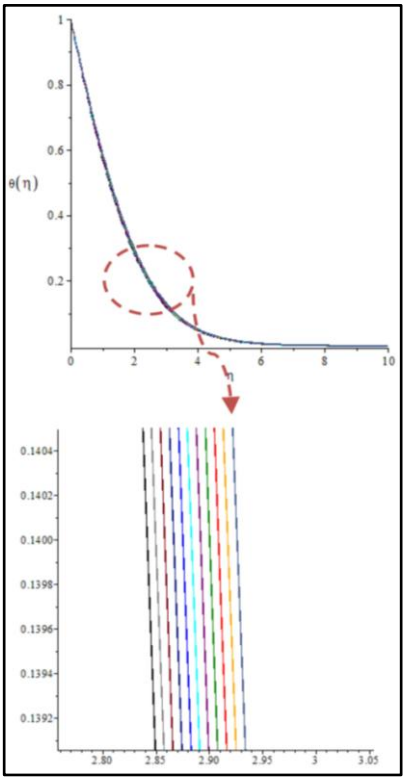

Fig. 11. Effect of ϕ on velocity distribution *θ(η)* in the case of Ag-water

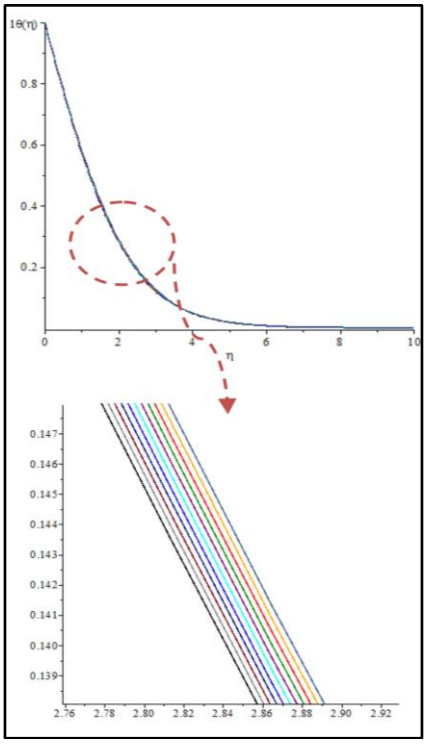

Fig. 13. Effect of ϕ on velocity distribution *θ(η)* in the case of Al_2O_3-water

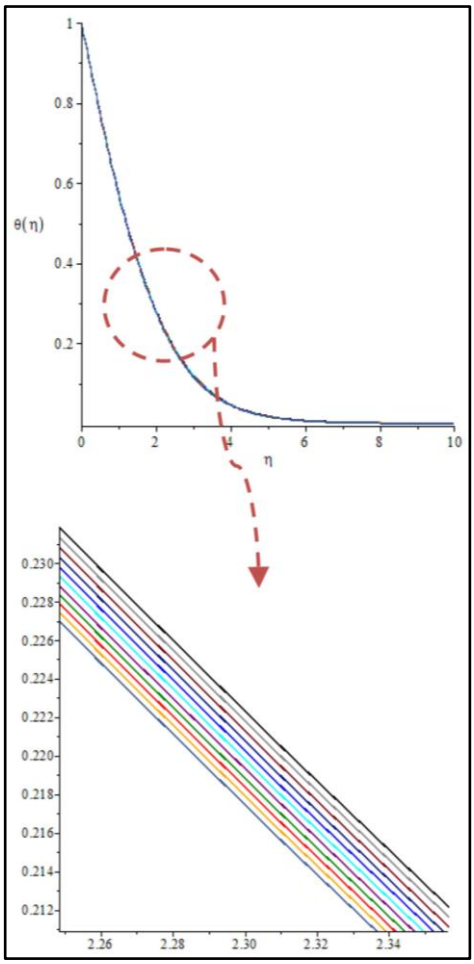

Fig. 14. Effect of ϕ on velocity distribution $\theta(\eta)$ in the case of TiO_2-water

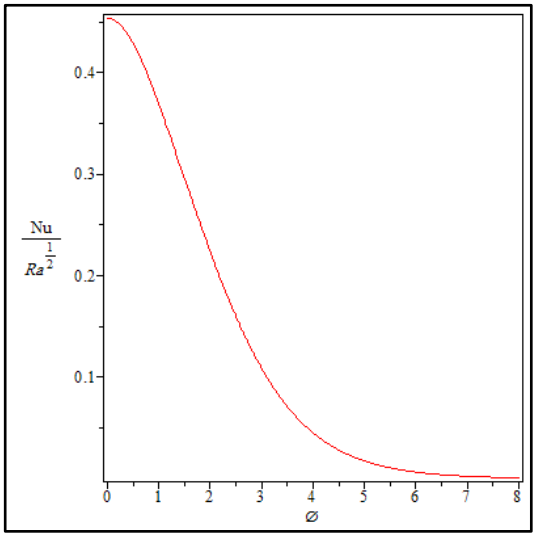

Fig. 15. Effects of the nanoparticle volume fraction ϕ on dimensionless heat transfer rates in the case of Cu-water

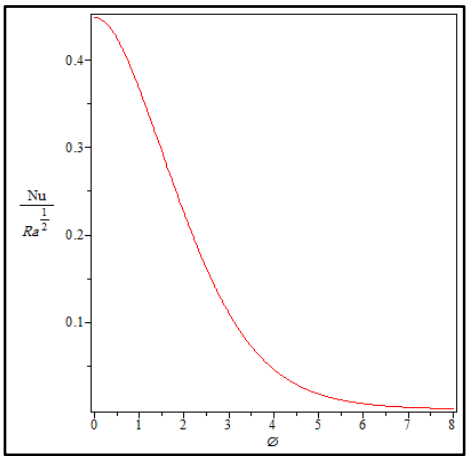

Fig. 16. Effects of the nanoparticle volume fraction ϕ on dimensionless heat transfer rates in the case of Ag-water

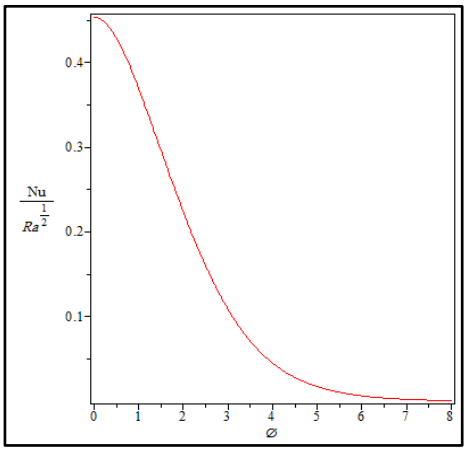

Fig. 17. Effects of the nanoparticle volume fraction ϕ on dimensionless heat transfer rates in the case of Al_2O_3-water

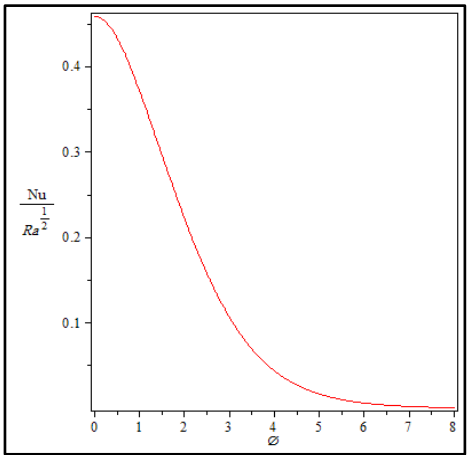

Fig. 18. Effects of the nanoparticle volume fraction ϕ on dimensionless heat transfer rates in the case of TiO_2-water

We can show that the change of the velocity distribution when we use different types of nanoparticles from Figure 19, which depict the Ag-nanoparticles are the highest when the base fluid is water and when ϕ =0.25. Thus the presence of the nanoparticles volume fraction increases the momentum boundary layer thickness. Moreover Figure 20 displays the behavior of the different types of nanoparticles on temperature distribution when ϕ =0.25. The figure showed that by using different types of nanofluid as the values of the temperature change and the Ag-nanoparticles are the upper distribution.

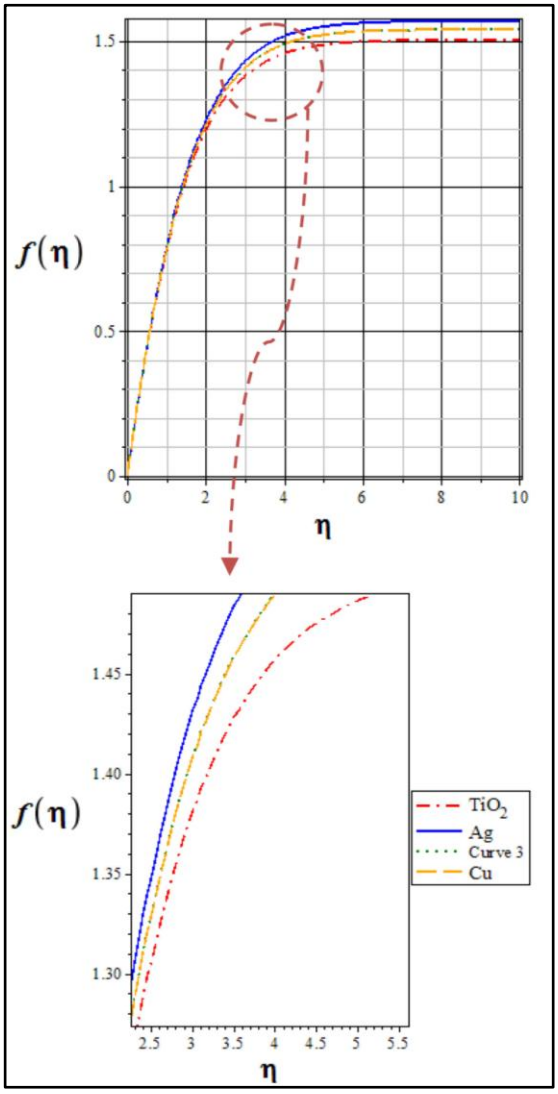

Fig. 19. velocity distribution *f (η)* for different type of nanofluids when ϕ =0.25

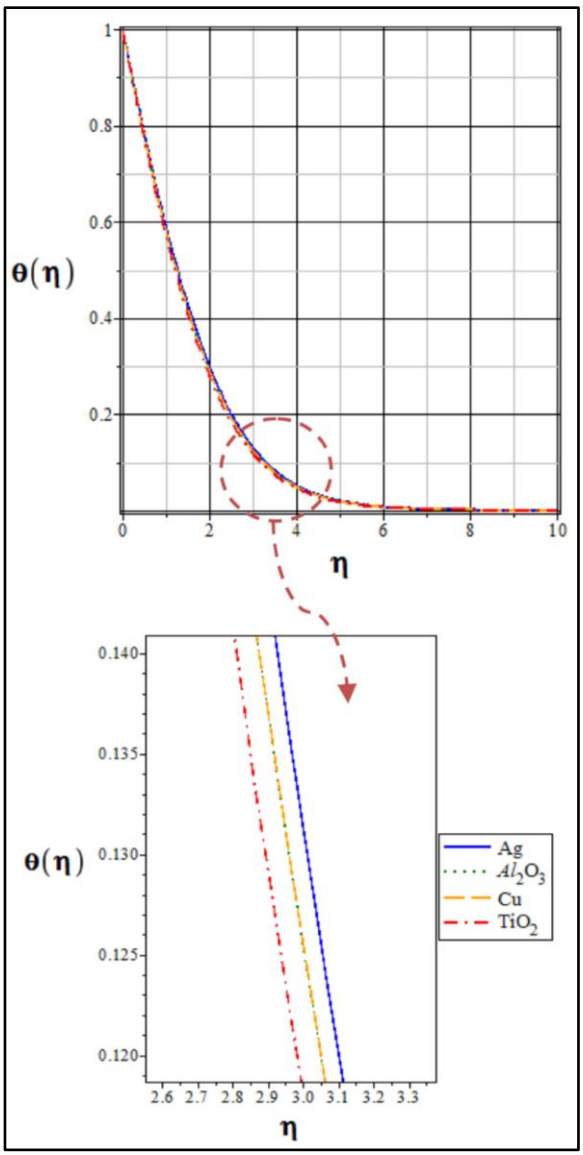

Fig. 20. Temperature profiles *θ(η)* for different type of nanofluids when ϕ =0.25

Figures 15-18 shows the variation of the reduced Nusselt number with the nanoparticles volume fraction ϕ for the selected types of the nanoparticles. It is clear that the heat transfer rates decrease with the increase in the nanoparticles volume fraction ϕ. The change in the reduced Nusselt number is found to be lower for higher values of the parameter ϕ. It is observed that the reduced Nusselt number is higher in the case of Ag-nanoparticles and next nanoparticles, TiO_2-nanoparticle and Al_2O_3-nanoparticles. Also, the Figures 11-14 and Table 2 shows that the values of

θ′(0) change with Newtonian nanofluid changes, namely we can say that the shear stress and heat transfer rate change by taking different types of nanofluid. Furthermore this depicts that the Newtonian nanofluids will be very important materials in the heating and cooling processes. Figures 21-24 shows that the with assumption of spherical nanoparticles, with increases diameter of the nanoparticles and with decreases vertical cone angle (γ) so increases nanofluids Darcian velocity component And It is observed that the increases nanofluids Darcian velocity component is higher in the case of Ag-nanoparticles.

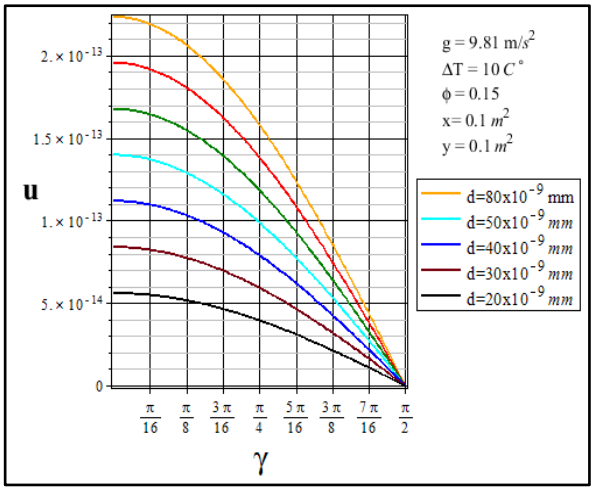

Fig. 21. Effect of γ (half angle of the cone) on u(Darcian velocity component) in the case of Ag-water

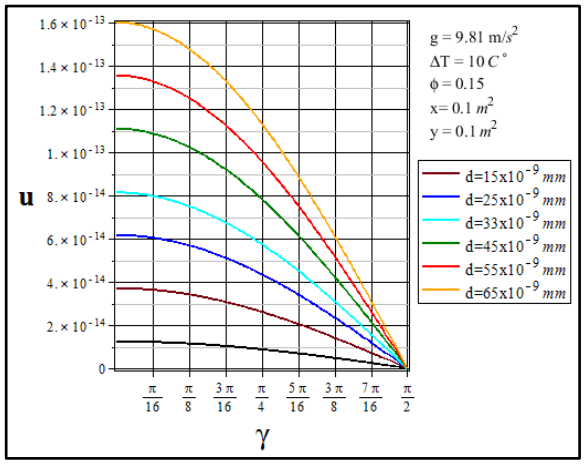

Fig. 22. Effect of γ (half angle of the cone) on u (Darcian velocity component) in the case of Al_2O_3-water

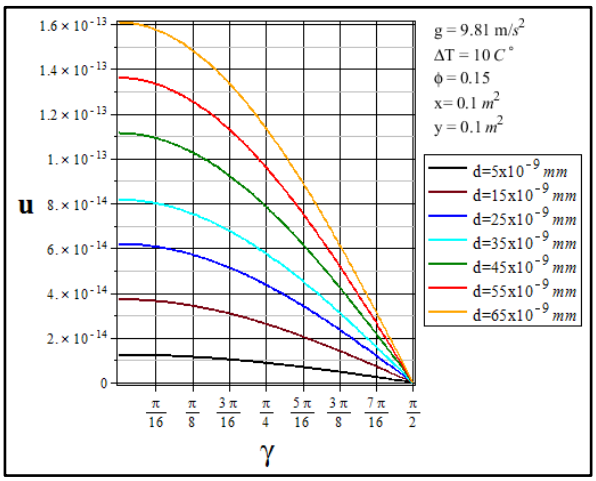

Fig. 23. Effect of γ (half angle of the cone) on u (Darcian velocity component) in the case of TiO_2-water

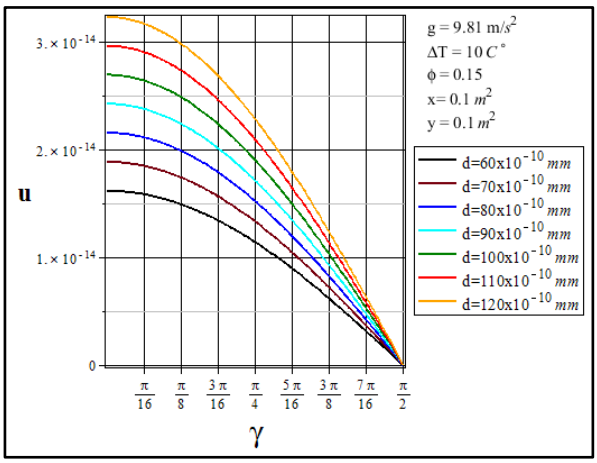

Fig. 24. Effect of γ (half angle of the cone) on u (Darcian velocity component) in the case of Cu -water

CONCLUSIONS

The problem of steady free convection boundary layer flow of Newtonian nanofluid past a vertical cone embedded in porous medium was studied. The effects of solid volume fraction (ϕ) on the flow and heat transfer characteristics of four types of nanofluids, namely, the dispersion of Copper (Cu), Silver (Ag), Alumina (Al_2O_3) and Titanium oxide (TiO_2), in water as the base fluid, were determined. As expected, increasing the volume fraction of nanoparticles, lead to an increase the velocity of temperature profiles and a

decrease of the Nusselt number. Ag-nanoparticles exhibited the highest cooling performance, while Al_2O_3-nanoparticles resulted in highest heating performance.

REFERENCES

[1] Ingham D. B., Pop I., (2002), Transport Phenomena in Porous Media Pergamon Press: Oxford

[2] Nield D. A., Kuznetsov A. V., (2008), Natural convection about a vertical plate embedded in a bidisperse porous medium. *Int. J. Heat Mass Transf*. 51: 1658–1664.

[3] Mahdy A., Hady F. M., (2009), Effect of thermophoretic particle deposition in non-Newtonian free convection flow over a vertical plate with magnetic field effect. *J. Non-Newtonian Fluid Mech*. 161: 37–41.

[4] Ibrahim F. S., Hady F. M., Abdel-Gaied S. M., Eid M. R., (2010), Influence of chemical reaction on heat and mass transfer of non-Newtonian fluid with yield stress by free convection from vertical surface in porous medium considering Soret effect. *Appl. Math. Mech. -Engl. Ed.* 31: 675–684.

[5] Yih K. A., (1999), Coupled heat and mass transfer by free convection over a truncated cone in porous media. VWT/VWC or VHF/VMF. *Acta Mech*. 137: 83–97.

[6] Murthy PVSN., Singh P., (2000), Thermal dispersion effects on non-Darcy convection over a cone. *Comp. Math. Applic*. 40: 1433–1444.

[7] Roy S., Anilkumar D., (2004), Unsteady mixed convection from a rotating cone in a rotating fluid due to the combined effects of thermal and mass diffusion. *Int J. Heat Mass Transf*. 47: 1673–1684.

[8] Takhar H. S., Chamkha A. J., Nath G., (2004), Effect of thermophysical quantities on the natural convection flow of gases over a vertical cone. *Int. J. Eng. Sci*. 42: 243–256.

[9] Singh P. J., Roy S., (2007), Unsteady mixed convection flow over a vertical cone due to impulsive motion. *Int. J. Heat Mass Transf*. 50: 949–959.

[10] Kumari M., Nath G., (2009), Natural convection from a vertical cone in a porous medium due to the combined effects of heat and mass diffusion with non-uniform wall temperature/concentration or heat/mass flux and suction/injection. *Int. J. Heat Mass Transf*. 52: 3064–3069.

[11] Cheng C. Y., (2010), Nonsimilar boundary layer analysis of double-diffusive convection from a vertical truncated cone in a porous medium with variable viscosity. *Int. Comm. Heat Mass Transf*. 37: 1031–1035.

[12] Choi S. U. S., (1995), Enhancing thermal conductivity of fluid with nanoparticles. Developments and applications of non-Newtonian flow. *ASME FED* 231/MD. 66: 99–105.

[13] Khanafer K., Vafai K., Lightstone M., (2003), Buoyancy-driven heat transfer enhancement in a two-dimensional enclosure utilizing nanofluids. *Int. J. Heat Mass Transf*. 46: 3639–3653.

[14] Buongiorno J., (2006), Convective transport in nanofluids. *ASME J. Heat Transfer*. 128: 240–250.

[15] Daungthongsuk W., Wongwises S., (2007), A critical review of convective heat transfer nanofluids. *Ren. Sustainable Energy Rev*. 11: 797–817.

[16] Oztop H. F., Abu-Nada E., (2008), Numerical study of natural convection in partially heated rectangular enclosures filled with nanofluids. *Int. J. Heat Fluid Flow*. 29: 1326–1336.

[17] Nield D. A., Kuznetsov A. V., (2009), The Cheng–Minkowycz problem for natural convective boundary-layer flow in a porous medium saturated by nanofluids. *Int. J. Heat Mass Transf*. 52: 5792–5795.

[18] Nield D. A., Kuznetsov A. V., (2011), The Cheng–Minkowycz problem for the doublediffusive natural convective boundary-layer flow in a porous medium saturated by nanofluids. *Int. J. Heat Mass Transf.* 54: 374–378.

[19] Ahmad S., Pop I., (2010), Mixed convection boundary layer flow from a vertical flat plate embedded in a porous medium filled with nanofluids. *Int. Comm. Heat Mass Transf*. 37: 987–991.

[20] Khan W. A., Pop I., (2010), Boundary-layer flow of a nanofluid past a stretching sheet. *Int. J. Heat Mass Transf*. 53: 2477–2483.

[21] Kuznetsov A. V., Nield D. A., (2010), Natural convective boundary-layer flow of a nanofluid past a vertical plate. *Int. J. Thermal Sci*. 49: 243–247.

[22] Kuznetsov A. V., Nield D. A., (2010), Effect of local thermal non-equilibrium on the onset of convection in a porous medium layer saturated by a nanofluid. *Transp. Porous Media.* 83: 425–436.

[23] Bachok N., Ishak A., Pop I., (2010), Boundary-layer flow of nanofluids over a moving surface in a flowing fluid. *Int. J. Thermal Sci*. 49: 1663–1668.

[24] Dehghan M., Shakeri F., (2007) Solution of a partial differential equation subject to temperature over specification by He's homotopy perturbation method. *Physica Scripta*. 75: 778–787.

[25] Ziabakhsh Z., Domairry G., Esmaeilpour M., (2009), Solution of the laminar viscous flow in a semi-porous channel in the presence of a uniform magnetic field by using the Homotopy analysis method. *Comm. Nonlin. Sci. Num. Simul*. 14: 1284-1294.

[26] Ziabakhsh Z., Domairry G., (2009), Analytic solution of natural convection flow of a non-Newtonian fluid between two vertical flat plates using Homotopy analysis method. *Nonlinear Sci*. 14: 1868-80.

[27] Abbasbandy S., (2006), The application of homotopy analysis method to nonlinear equations arising in heat transfer. *Phys. Lett. A.* 360: 109–113.

[28] Abbasbandy S., (2007), The application of homotopy analysis method to solve a generalized Hirota–Satsuma coupled KdV equation. *Phys. Lett. A.* 361: 478–483.

[29] Liao S. J., (2006), Series solutions of unsteady boundary-layer flows over a stretching flat plate. *Stud. Appl. Math*. 117: 239–264.

Cite this article as: M. M. Peiravi *et al.*: Evaluation of the heat transfer rate increases in retention pools nuclear waste. ***Int. J. Nano Dimens.*** 6 (4): 385-398, Autumn 2015.